REPORT DOCUMENTATION PAGE

Form Approved
OMB No. 0704-0188

PLEASE DO NOT RETURN YOUR FORM TO THE ABOVE ADDRESS.

1. REPORT DATE *(DD-MM-YYYY)*	2. REPORT TYPE	3. DATES COVERED *(From - To)*
14-05-2007	FINAL	Jun - Dec 2006

4. TITLE AND SUBTITLE

Wind Tunnel and Water Channel Investigations for Improving MAV Aerodynamic Performance.

5a. CONTRACT NUMBER

FA9550-06-1-0490

5b. GRANT NUMBER

5c. PROGRAM ELEMENT NUMBER

6. AUTHOR(S)

Spedding, Geoffrey
Browand, Frederick
McArthur, John

5d. PROJECT NUMBER

5e. TASK NUMBER

5f. WORK UNIT NUMBER

7. PERFORMING ORGANIZATION NAME(S) AND ADDRESS(ES)

University of Southern California
University Park
Los Angeles, CA 90089-1191

8. PERFORMING ORGANIZATION REPORT NUMBER

9. SPONSORING/MONITORING AGENCY NAME(S) AND ADDRESS(ES)

Air Force Office of Scientific Research
Attn: Col. Rhett Jeffries
875 N. Randolph St
Room 3112
Arlington VA 22203-1954

10. SPONSOR/MONITOR'S ACRONYM(S)

AFOSR

11. SPONSOR/MONITOR'S REPORT NUMBER(S)

12. DISTRIBUTION/AVAILABILITY STATEMENT

Distribution is unlimited, unclassified.

AFRL-SR-AR-TR-07-0498

13. SUPPLEMENTARY NOTES

14. ABSTRACT

Extensive investigations of the role of sweep in generating and/or stabilizing a leading edge vortex (LEV) in low Reynolds number (Re = 10 000) aerodynamics were made by tracing dye over wing shapes in a low-turbulence water channel. Unlike any other experiment to date, the variation in sweep was the only parameter change, all others being fixed. The airfoil shape was a cambered plate, which is close to optimal at such Re. LEVs are not generated readily and are unlikely to be significant contributors to aerodynamic performance in fixed wing aircraft at this Re. The flows are complex and almost always involve significant spanwise components. The results are being used to guide current wind-tunnel based quantitative flow investigations in selected two-dimensional planes.

15. SUBJECT TERMS

16. SECURITY CLASSIFICATION OF:			17. LIMITATION OF ABSTRACT	18. NUMBER OF PAGES	19a. NAME OF RESPONSIBLE PERSON
a. REPORT	b. ABSTRACT	c. THIS PAGE			Geoffrey Spedding
U	U	U	UU	14	19b. TELEPHONE NUMBER *(Include area code)* (213) 740 7182

Wind Tunnel and Water Channel Investigations for Improving MAV Aerodynamic Performance

Geoff Spedding, Fred Browand, John McArthur
Aerospace and Mechanical Engineering
University of Southern California

Final Report for USC Contract# 53-4514-8161

From

Air Force Office of Scientific Research

Date submitted: May 14th 2007

The following report describes a series of detailed water channel measurements on swept wings at moderate Re = 5 000. The report refers to a database of image and movie files which have been provided to our local contract monitor, Michael Ol. Copies of this CDROM are available within AFOSR upon request.

1) Introduction

Many studies on biological flying systems have revealed that a dominant feature of the flow physics of a flapping wing at low to moderate Reynolds numbers (Re) is the formation of a leading edge vortex (LEV).[1,2,3] The LEV forms due to the separation at the sharp leading edge and in three-dimensional geometries transports fluid from the wing-center towards the wing-tip. Although the ideas began in the insect flight community, an LEV was reported in a water channel experiment on a brass model of the swept wing of a Swift. For $3.7 \times 10^3 < Re < 3.7 \times 10^4$ PIV measurements showed that the 60û swept hand-wing of the Swift develops an LEV at an angle of attack, $\alpha = 10$û, and it was speculated that the LEV may cause an increase in lift.[4] However, later studies on real swift wings mounted on a force balance in a wind tunnel show that the LEV appears only at $\alpha > 30$û and for large sweep angles that exceed those used in nature, and does not provide an increase in lift.[5]

The LEV on a swept wing at these Re has been compared to the LEV generated on a delta wing, but no experiments have been done to test this comparison. In fact, there has been no study of a simple wing, where the only design parameter that is varied is the sweep. All studies have included non-zero taper, as well as aspect ratio and area changes while measuring the LEV. The primary purpose of the present experiments is to determine the effect of sweep on simple cambered wings at these low Re. The results should explain the conditions under which an LEV forms, and they will help guide further, more detailed studies of swept wings.

2) Methods

Dye injection experiments were conducted on swept, cambered plate wings at low Reynolds numbers (Re), in the USC water channel. Four wings were made of 0.08 cm thick brass shim stock, each with a 4.45 cm chord, 5% circular-arc cambered cross-section and sweep angles: $\Lambda = 0$û, 20û, 40û, 60û, as seen in figure 1. Each wing has an aspect ratio of 6, an area of 119 cm^2, a thickness ratio of 1.8% (0.08/4.45), and no taper. The wings were made by rolling the shim stock to the specified camber, then soldering each half of the wing together. The sting (support mount) was made by stacking 3 pieces of the same brass shim stock together. It was soldered to the wings in the center of the wing (at the apex). The chord-wise dimension of the sting was 3.4 cm. The water channel setup is shown in figure 2.

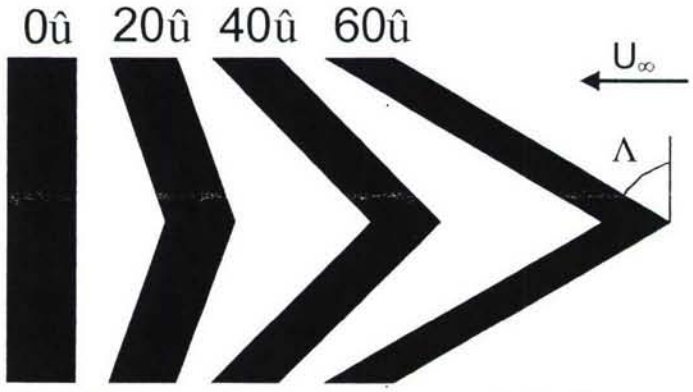

Figure 1. Planform geometry of wings tested. The streamwise chord length is constant.

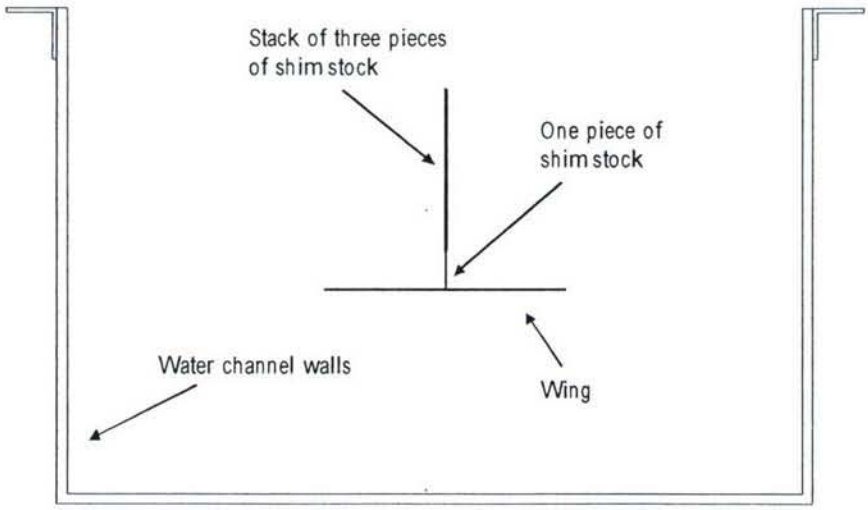

Figure 2. Streamwise view of water channel setup.

The dye was injected 16 cm upstream of the wings using a syringe pump and a 0.16 cm outside diameter, 0.1 cm inside diameter tube. The tube extended vertically into the water channel, with a 4 cm bend radius near the end, and a 2 cm horizontal section after the bend. The water channel was set to a nominal speed of 10 cm/s, which made the chord-based $Re = 5 \times 10^3$. This choice of dye injection tubing and water channel speed provided enough stiffness in the tubing so that it did not bend, and has a laminar boundary layer flow inside and outside the tube, so that the dye streak was steady. The bend radius was large enough so that the vortex shedding of the vertical tube did not affect the dye streak. The angle of attack (α) was varied between a nominal 0û and 20û in 2.5û increments.

Images and video were taken using a Sony CyberShot digital camera with manual and automatic mode to allow fine-tuning of the image acquisition parameters. Low temperature compact fluorescent lamps (CFL) were used to light the water channel test section. Images were taken from the right-side of the wing (looking upstream) and from various angles around the wing. Images were later analyzed to provide a better estimate of α, with less than 1û uncertainty.

After analysis of the data, the most significant of the flow features can be identified, and these are presented in the current document. Included with this report is a CD containing images and videos of the most interesting of the cases studied (a DVD containing all the cases is available). All images and videos on the CD can all be viewed on standard software using the XviD Mpeg-4 Compression Codec. The naming convention is as follows:

Lxx – Sweep angle of the wing (Λ), xx, in degrees
axx – Nominal geometric angle of incidence of the wing (α), xx, in degrees
yxx – Span-wise location of the dye, xx, in % of the span away from the wing-center

All references to images and videos will be in the format of "directory" / "image number" (ie. L00_a03_y50/00142 is used to indicate image number 00142 in the directory that contains images of the wing with sweep of zero degrees, at angle of attack 3 degrees, and with the dye at 50% of the span away from the wing center). Throughout this report, the wing-center will refer to the y00 location of the wing (which is the plane of symmetry of the wing), the mid-wing will refer to the y25 location of the wing (half way to the wing-tip), and the wing-tip will refer to the y50 location of the wing (the end of the wing). All angles of attack used in this report are nominal angles of attack. The actual angle of attack as measured using the images is available upon request.

3) Results

3.1) Non-Swept Wings

At low α, the non-swept wing wake is an orderly array of alternating signed vortices, there is a strong wing-tip vortex at moderate angles of incidence, and separation begins early on the wing at high α. Two features are unusual: the span-wise flow along the trailing edge at moderate α, and the three-dimensional nature of large scale separation.

3.1.1) Span-wise flow along the Trailing Edge

A span-wise flow travels along the trailing edge (TE) from the wing-tip towards the wing-center. This occurs at $3° \leq \alpha \leq 8°$, and only the dye at the wing-tip is entrained into this flow, the dye at the mid-wing is not. While the flow travels towards the wing-center, it travels slightly up and down the chord within the separated region near the TE. This forms a wave-like pattern along the TE. The phenomenon is sketched in figure 3, and seen in the following images and movies:

L00_a03_y50\00142
L00_a05_y50\00183-7
L00_a08_y50\00258-9;00266-8;MOV 00260-1

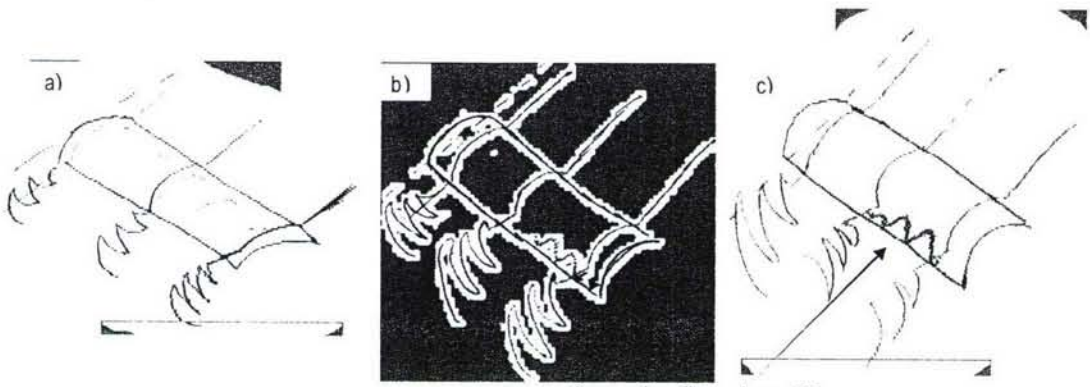

Figure 3. Sketches of the upper surface flow on a non-swept wing at a) $\alpha=0°$ b) $\alpha=3°$ and c) $\alpha=5°$

The dye visualizations at y00 and y25 show that the flow at the wing-center and at the mid-wing are both attached until very near the TE. The flow from the wing-tip towards the wing-center is most likely traveling in the separated region of the wing. This wave-like pattern in the separated region is unexpected and not well documented in the literature. In addition to being related to the separated region of the wing, it may also be affected by the wing-tip vortex.

3.1.2) Three dimensional separation

The TE flow towards the wing-center exists up to $\alpha = 8°$, but after that the flow is no longer constrained to a region near the TE. At $\alpha = 10°$ the dye travels from the TE of the wing-tip, up the chord nearly to the leading edge (LE), and towards the wing-center nearly to the mid-wing. This α is also when full separation at the mid-wing, and wing-center locations occur. It is not clear whether the flow at the wing-tip is being "pushed" by the wing-tip vortex, or whether the separation at the mid-wing is "pulling" the flow at the wing-tip back up the chord. Figure 4 sketches the difference between the flow at $\alpha = 8°$ and $\alpha = 10°$. The following images and movies are relevant:

L00_a10_y00\00297-302;MOV00305
L00_a10_y25\00318-21;MOV00322a-c
L00_a10_y50\MOV 00341

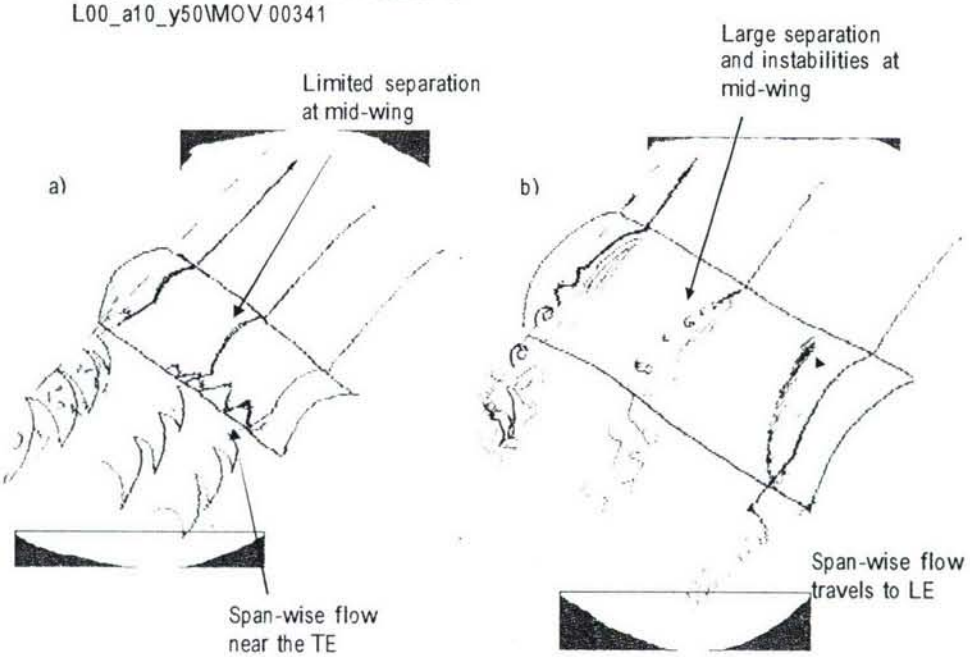

Figure 4. Sketches of the flow around a non-swept wing at a) $\alpha=8°$ b) $\alpha=10°$

These results compare well with corresponding USC wind tunnel tests on 3% thick, 5% cambered plate airfoils with aspect ratio 6 and Re = 11.5 x 10^3. Force balance measurements across a large range of α (fig. 5) show that for the cambered plate, 8ûis the last α with high lift-to-drag ratio (L/D). After that, there is a significant decline, and this is illustrated by the flow separation over much of the wing found in the present water channel experiments. Raw images of particles taken during DPIV experiments (fig. 6) also indicate a change in the flow field over this range of α. However, it is impossible to see 3D effects. For this type of understanding, one must use techniques capable of visualizing all 3 components of the velocity in a volume.

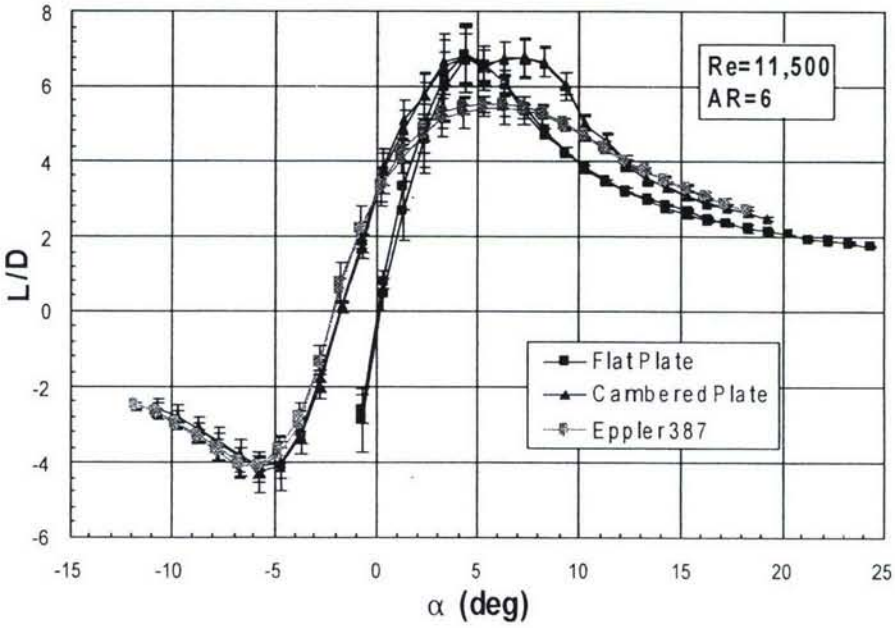

Figure 5. Lift-to-drag ratio of three airfoil geometries, at aspect ratio 6 and Re11.5k. Both loading and unloading cases are plotted, and there is no significant difference. Uncertainties are estimated by the standard deviation of 4 independent measurements.

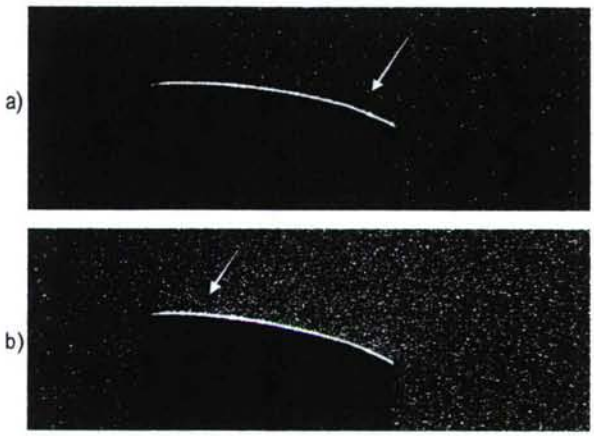

Figure 6. DPIV images taken at α= 7 ûand 10ûfor a) and b) respectively. The bright curved line is the glare on the upper surface of the cambered wing illuminated by the laser. There is a dark line extending from the surface of the wing (indicated by the arrow) that marks the separation line.

3.2) SWEPT WINGS

3.2.1) Span-wise flow direction reversal

Comparing non-swept wings to swept wings, the most obvious change is in the flow along the TE mentioned above. For non-swept wings, this flow always begins at the wing-tip TE, travels near the TE (within the separated region of the wing), and along the span towards the wing-center in a wave-like pattern. Even at the smallest sweep angle studied (Λ = 20û) the direction of this flow is reversed, and instead of originating at the wing-tip, it originates instead at the wing-center. The flow is still constrained to be near the TE, and it also exhibits a wave-like pattern. The wave-length changes, however, as the sweep angle changes, and the angle of incidence at which this flow occurs also changes. This is demonstrated for each sweep angle in figure 7, and in:

L20_a05_y25\01309-11;01320;MOV0 1308
L20_a08_y25\01370-2;01455-9;MOV 01373a-b;MOV0146 0a-b
L40_a08_y00\00827
L40_a10_y25\00987-9;MOV00976
L40_a13_y25\01028-35;MOV01027
L60_a05_y00\02011-5;MOV02002
L60_a08_y00\02087-93;MOV02086
L60_a10_y00\02155-8;02166;02171-2;MOV02143;MOV0 2146b;MOV02174

The fact that there is span-wise flow along the TE is not surprising, but the coherent and organized structure is somewhat unexpected. Also, the separation at the mid-wing occurs closer to the LE when compared to the separation at the wing-center. This span-wise flow from the wing-center is most likely causing this increased separation.

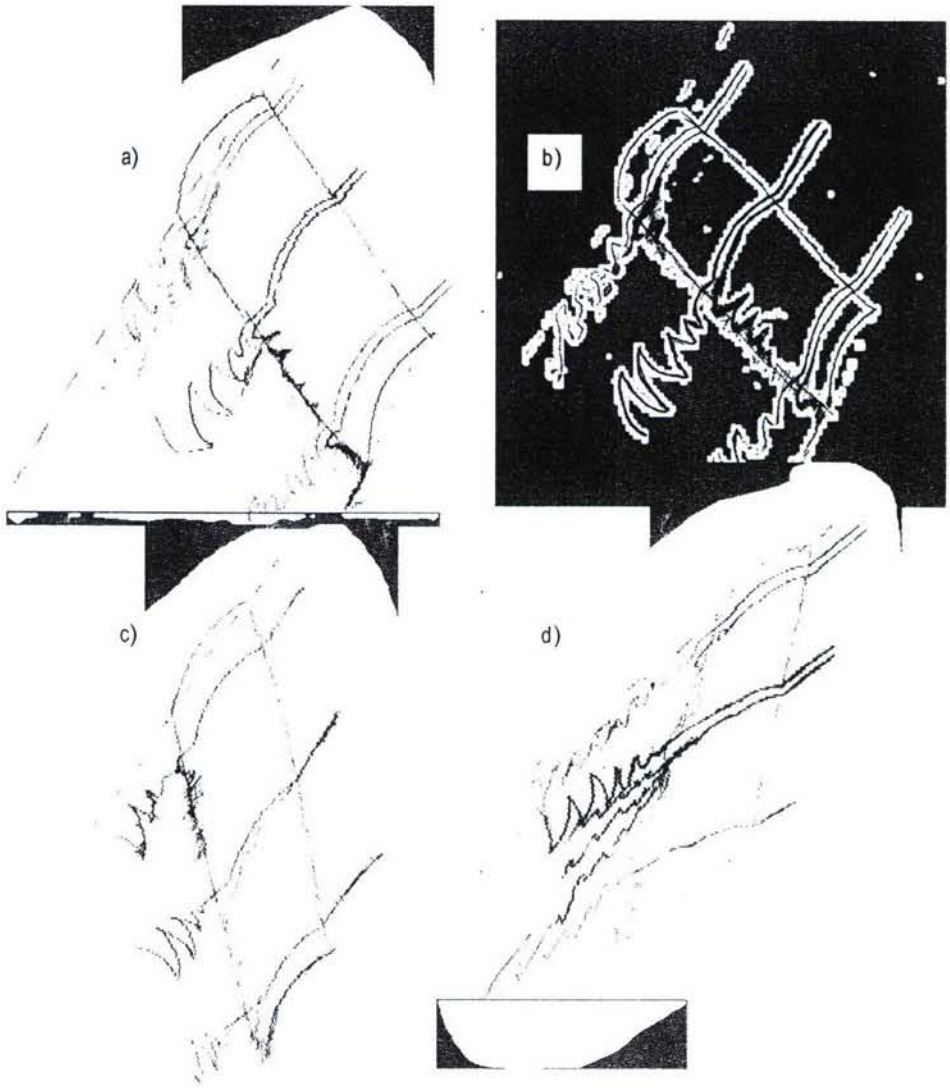

Figure 7. Sketches of the flow around a wing at a) Λ=20ûα=5ûb) Λ=20ûα=8ûc) Λ=40ûα=13ûd) Λ=60ûα=5û

3.2.2) Separation process reversal

The separation process of a swept wing is also in the reverse direction of the separation process of a non-swept wing. The non-swept wing has been described earlier in this paper; separation originates from the wing-tip and causes separation at the mid-wing and wing-center. For a swept wing, the separation starts at the center-wing and then causes large scale separation at the mid-wing and wing-tip. The sketches in figure 8 demonstrate this, as do files:

L20_a08_y00\01424;01431-4;01442;MOV1435
L20_a08_y25\01470-6;01454-9;01370-5;MOV01460a-b
L20_a08_y50\01396-400;MOV01398
L20_a10_y00\01509;01512-4;MOV01 516;MOV01524
L20_a10_y25\01533-40;01548;MOV0 1556a-b
L20_a10_y50\01566-9;01576-80;MO V01583
L20_a13_y00\01604-9;MOV01610a-b
L20_a13_y25\01623-31;MOV01634
L20_a13_y50\01650-5;01659;MOV01 643;MOV01660
L40_a15_y00\01052-5;MOV01056a-0 1057
L40_a15_y25\01062-6;MOV01067a-b
L40_a15_y50\01074;01078;MOV0107 7
L60_a13_y00\02233-7;02242;MOV02 238a
L60_a13_y25\02257-60;02272-5;02281-4;02290-1;02294-5;MOV02261-3
L60_a13_y50\02304-8;02315-8;MOV 02319

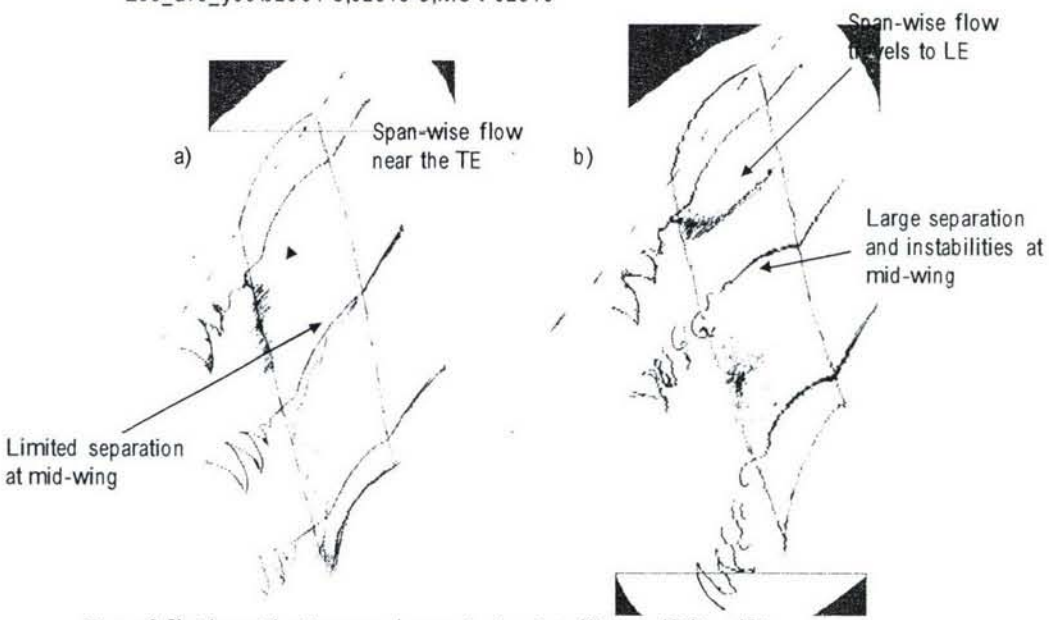

Figure 8. Sketches of the flow around a swept wing at Λ=40û a) α=13ûb) α=15û

Separation at the mid-wing is related to a change in the spanwise flow. Before separation at the mid-wing, the spanwise flow is constrained to a region near the TE. After separation at the mid-wing, the span-wise flow travels from the TE nearly to the LE. Again, it is unclear whether the mid-wing separation causes the span-wise flow to curl upstream, or whether the strong shear layer at the wing-center curls the spanwise flow upstream and thus causes mid-wing separation. It is clear however, that the separation is highly three-dimensional.

3.2.3) Wing-center wake

The wake of swept wings is also quite different from non-swept wings. One difference is that the wake at the wing-center is more regular at moderate α than at $\alpha \sim 0$. The wake at the wing-center of swept wings at small α is quite disorganized compared to the non-swept wing. The swept wing vortex street has a number of distinct frequencies, and it seems to be three-dimensional, while the non-swept wing has a single frequency and is very planar. As α increases to 5-10 degrees, the wake of the swept wing becomes more planar and has a dominant frequency, whereas the non-swept wing begins to lose its regularity in this range. Figure 9 shows sketches of the 20ûswept wing from α = 0û-10û and the following images and movies show the regular wakes:

L00_a00_y00\00060-1;00065-8
L00_a05_y00\00145-6;00148-55
L00_a10_y00\00284-8;00292-4;00297-9;MOV00289
L20_a00_y00\01148-52;01156-9;MO V01160a-b
L20_a05_y00\01285-7;MOV01188a-b
L20_a10_y00\01504-8;MOV1507a-b
L40_a05_y00\00805-10;00816;MOV0 0811a-b
L40_a10_y00\00942-9;MOV00946
L40_a15_y00\01050-1;MOV01056c
L60_a03_y00\01897-902;MOV01898; MOV01904
L60_a08_y00\02079-82;MOV02083-4
L60_a13_y00\02232-3;MOV2238b

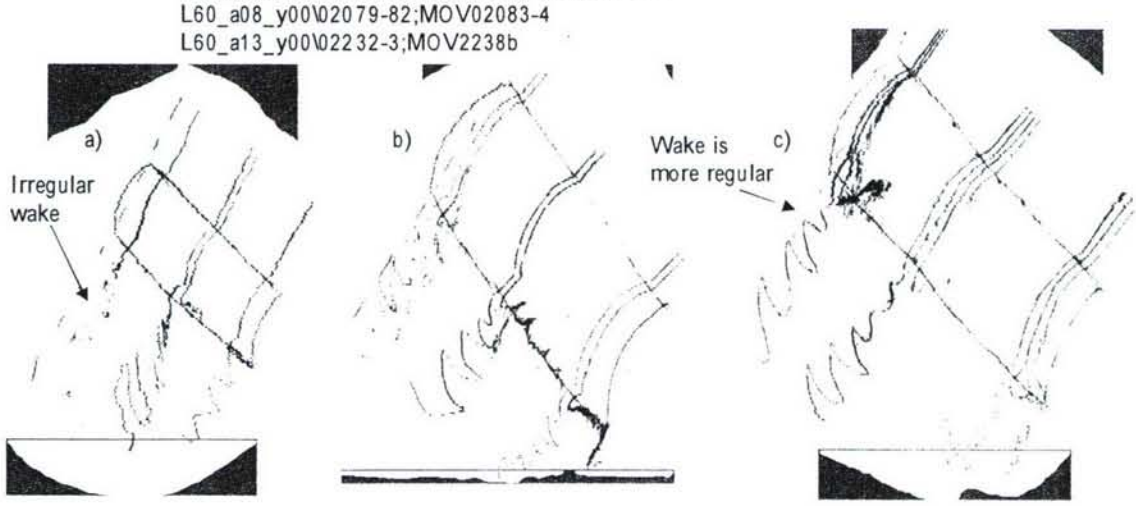

Figure 9. Sketches of the flow around a swept wing at Λ=20û a) α=0ûb) α=5ûc) α=10û

The wake regularization at higher α is most apparent at the moderate sweep angle of 20û. As sweep angle increases to 40 and 60û, the wake becomes vertically thinner and has more stream-wise vorticity in it.